# Supplemental Material

**Anti-GRP78 autoantibodies induce endothelial cell activation and accelerate the development of atherosclerotic lesions**

Elizabeth D. Crane[1*], Ali A. Al-Hashimi[2,3*], Jack Chen[2], Edward G. Lynn[2], Kevin Doyoon Won[2], Šárka Lhoták[2], Magda Naiem[2], Khrystyna Platko[2], Paul Lebeau[2], Jae Hyun Byun[2], Bobby Shayegan[3], Joan Krepinsky[2], Serena Marchiò[4,5], Renata Pasqualini[6,7], Wadih Arap[6,8] and Richard C. Austin[1,2]

Departments of [1]Biochemistry and Biomedical Sciences and [2]Medicine, Division of Nephrology. [3]Division of Urology, Department of Surgery, McMaster University, McMaster University and The Research Institute of St. Joseph's, Hamilton, Ontario, Canada. [4]Department of Oncology, University of Turin, 10060 Candiolo, Italy, and [5]Candiolo Cancer Institute, Fondazione del Piemonte per l'Oncologia (FPO)-Istituto di Ricerca e Cura a Carattere Scientifico (IRCCS), 10060 Candiolo, Italy [6]Rutgers Cancer Institute of New Jersey at University Hospital, Newark, New Jersey 77103, USA. [7]Division of Cancer Biology, Department of Radiation Oncology, Rutgers New Jersey Medical School, Newark, New Jersey 77103, USA. [8]Division of Hematology/Oncology, Department of Medicine, Rutgers New Jersey Medical School, Newark, New Jersey 77103, USA.

**Supplemental material**

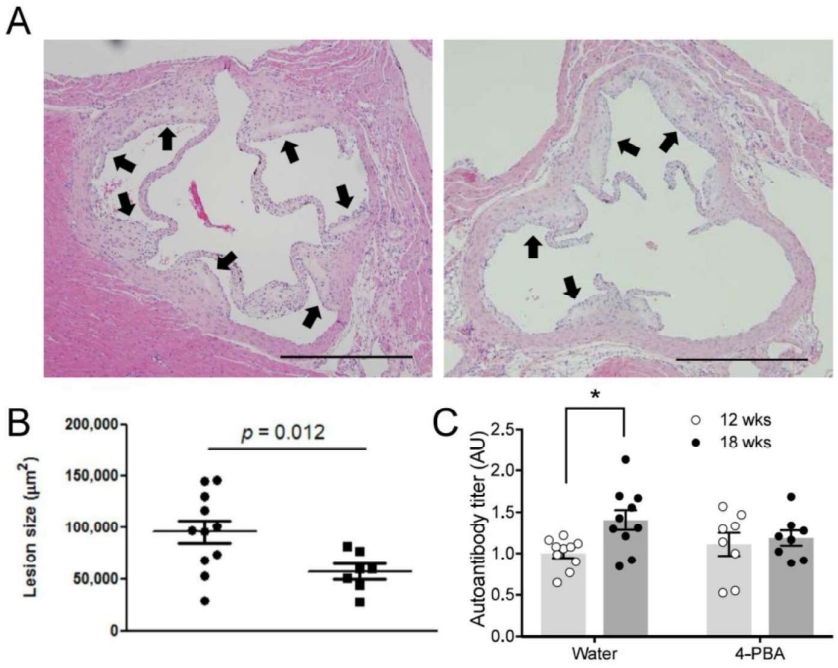


**Supplemental Figure 1.** 4-PBA suppresses lesion development and rise in anti-GRP78 autoantibody titers. (A-B) 17 weeks old; 11 weeks 4-PBA treatment (from 6 to 17 weeks of age). (C) Circulating GRP78a-Abs were measured by ELISA in mice given water only (Water) or water supplemented with 2.5 g/kg/day 4-PBA for 5 weeks. Baseline blood draws were taken at 12 weeks of age and after treatment (18 weeks of age). Data are presented as a ratio of absorbance units (AU) relative to a standard sample. n = 8-10 per group.

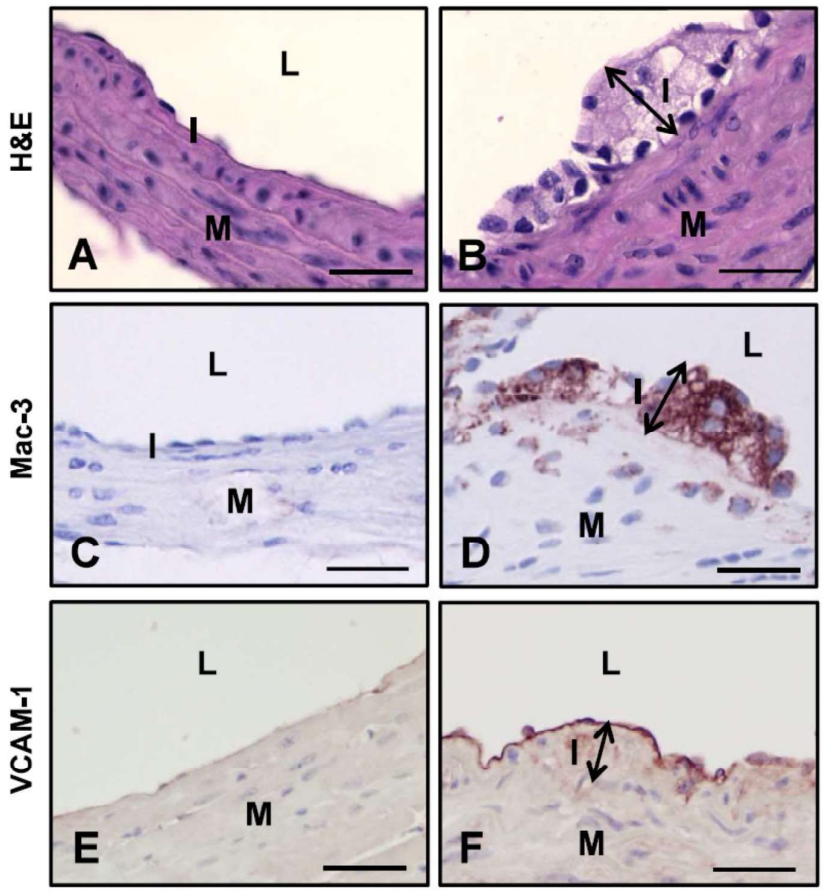


**Supplemental Figure 2.** Representative images of early atherosclerotic lesions from apoE$^{-/-}$ mice. Hematoxylin-and-eosin (H&E) staining of sections from the aortic root of 9-week-old, chow fed apoE$^{-/-}$ mice without (A) or with (B) early atherosclerotic lesions containing neointimal thickening. Intimal fatty streaks containing Mac-3-positive macrophages were observed in early lesions (D) but not in adjacent regions containing histologically normal vessel walls (C). Positivity of the endothelial layer for VCAM-1 was also increased in early lesions (F), compared to adjacent, normal vessel wall (E). L, lumen. M, media. I, intima (double arrow). Bar = 50 μm.

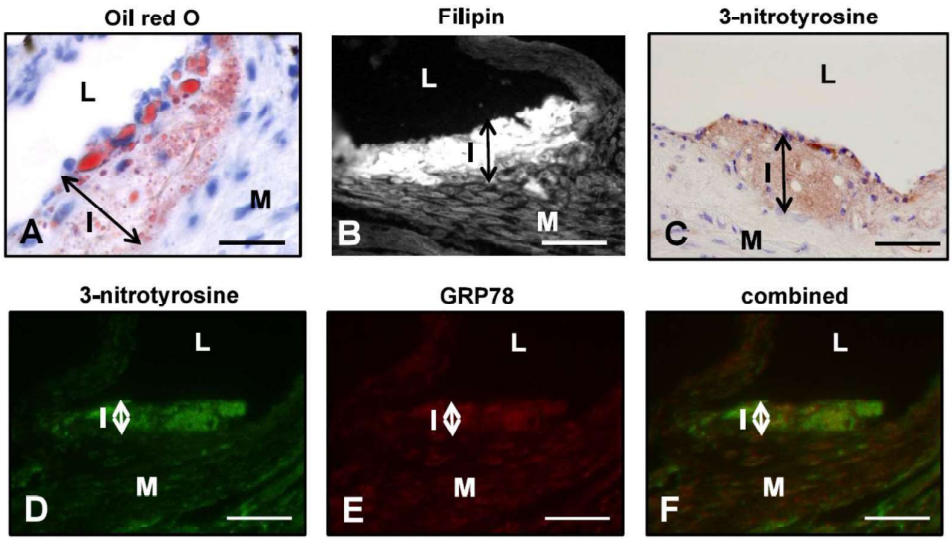


**Supplemental Figure 3.** Identification of ER stress-inducing agents in early atherosclerotic lesions from apoE$^{-/-}$ mice. Representative images of aortic root sections from 9-week-old, chow fed apoE$^{-/-}$ mice stained with either oil red O for neutral lipids (A), filipin for free cholesterol content (B) or immunostained for 3-nitrotyrosine to detect peroxynitrite-mediated nitrosative stress (C). Colocalization of 3-nitrotyrosine and GRP78 in lesion-resident macrophages from early atherosclerotic lesions (D-F). L, lumen. M, media. I, intima (double arrow). Bar = 50 μm.

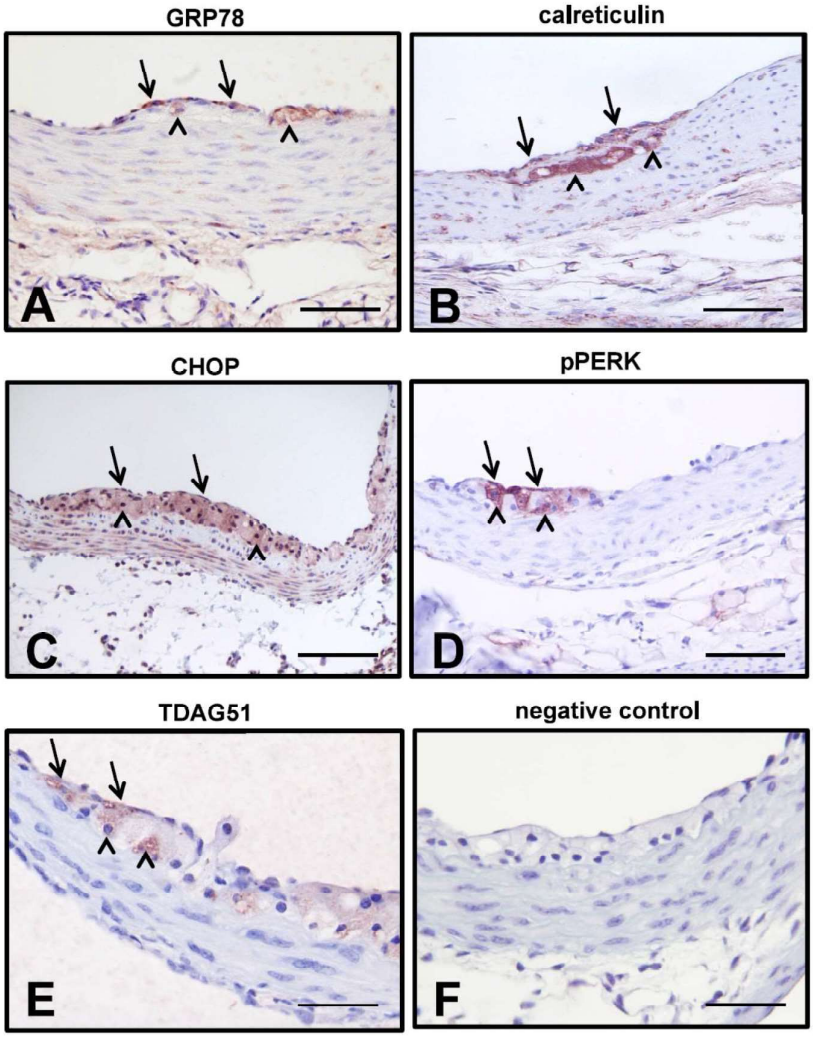


**Supplemental Figure 4.** Increased ER stress in early atherosclerotic lesions from apoE$^{-/-}$ mice. Representative images of aortic root sections from 9-week-old, chow fed apoE$^{-/-}$ mice immunostained for GRP78 (A), calreticulin (B), CHOP (C), phospho-PERK (D), TDAG51 (E) or secondary only control (F). Arrows represent positive immunostaining in the EC layer. Arrowheads represent immunostaining of intimal macrophages and macrophage foam cells. Immunostaining for these ER stress markers was absent or markedly reduced in the vessel wall adjacent to the early lesions. Bar = 50 μm.

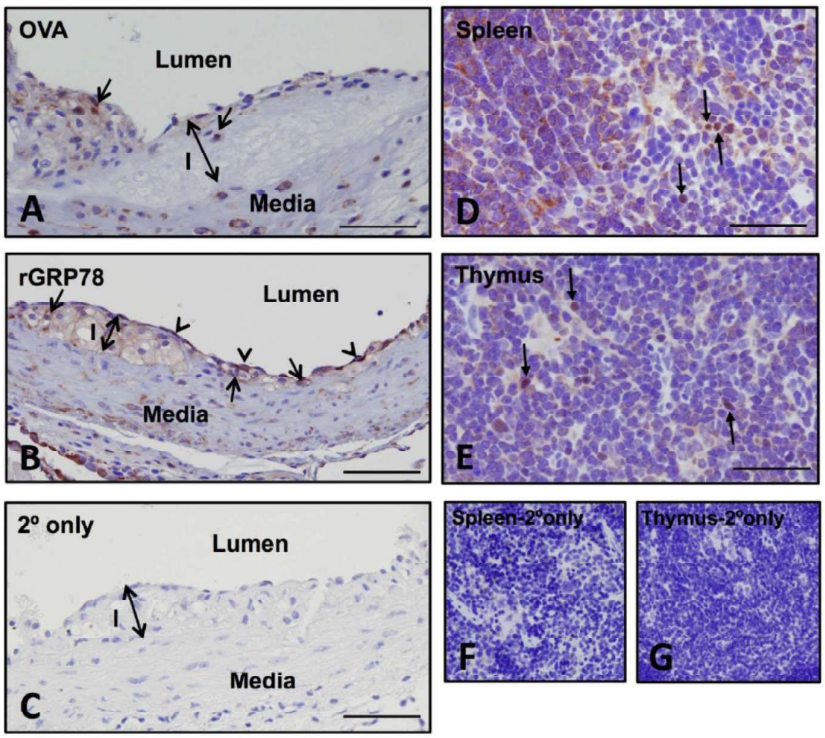


**Supplemental Figure 5. NFκB in atherosclerotic lesions from apoE$^{-/-}$ mice immunized with OVA or rGRP78.** Sections from aortic atherosclerotic lesions of 12-week-old apoE$^{-/-}$ mice immunized with OVA (A) or rGRP78 (B) were immunostained for NFκB. Representative images indicate positive immunostaining for NFκB in both macrophages (arrows) and ECs (arrowheads). Intensity of immunostaining for NFκB was increased in apoE$^{-/-}$ mice immunized with rGRP78. (C) Representative image of aortic atherosclerotic lesion immunostained with secondary antibody only from apoE$^{-/-}$ mice immunized with rGRP78. (D) Positive immunostaining for NFκB in mouse spleen. Arrows indicate positive NFκB nuclear staining in splenocytes. (E) Positive immunostaining for NFκB in mouse thymus. Arrows indicate positive NFκB nuclear staining in thymocytes. (F,G) Negative controls (secondary antibody only) for spleen and thymus. Bar = 100 μm.

**Supplemental Table 1.** qPCR primers

| Gene | Forward Primer | Reverse primer |
|---|---|---|
| *ICAM1* | TATGGCAACGACTCCTTCT | CATTCAGCGTCACCTTGG |
| *VCAM1* | CCAGGTGGAGCTCTACTCATTCCC | GCCGGTCAAGGGGGTACACG |
| *β-actin* | ACTTGTCTTTCAGCAAGGACT | TTCACACGGCAGGCATAC |